European Journal of Nuclear Medicine and Molecular Imaging (2019) 46:838–847
https://doi.org/10.1007/s00259-018-4133-x

ORIGINAL ARTICLE

Diagnostic performance of real-time robotic arm-assisted ^{18}F-FDG PET/CT-guided percutaneous biopsy in metabolically active abdominal and pelvic lesions

Rajender Kumar[1] · Bhagwant Rai Mittal[1] · Anish Bhattacharya[1] · Harmandeep Singh[1] · Amanjit Bal[2] · Shelvin Kumar Vadi[1] · Ashwani Sood[1] · Gaurav Prakash[3] · Harjeet Singh[4] · Aman Sharma[5]

Received: 4 July 2018 / Accepted: 12 August 2018 / Published online: 30 August 2018

Abstract

Purpose To evaluate the feasibility and diagnostic performance of ^{18}F-FDG PET/CT-guided biopsy of abdominal and pelvic lesions with automated robotic arm (ARA) assistance.

Methods This prospective study included 114 patients (75 men, 39 women; mean age 51.3 ± 14.7 years, range: 18–90 years) who underwent PET/CT-guided biopsy of FDG-avid abdominal and pelvic lesions from October 2014 to December 2017. Of these patients, 54 had a prior inconclusive CT-guided biopsy. The biopsies were done with ARA assistance, and a real-time sample was obtained after confirming the position of the needle tip within the target lesion on PET/CT. Histopathology reports were reviewed to evaluate the diagnostic performance of the procedure. Clinical or imaging follow-up was done to confirm negative results.

Results The lesions were successfully targeted in 110 of the 114 patients (96.5%) and yielded a pathological diagnosis. Pathological diagnoses were confirmed in 50 of the 54 patients with a prior inconclusive biopsy. Of the 110 lesions, 82 were malignant, 20 were benign, and 8 showed minimal residual FDG uptake at the end of treatment and had no active disease even on clinical and imaging follow-up of at least 3 months. Findings were true-positive in 102 lesions, false-positive in none, true-negative in eight and false-negative in four. The procedure showed sensitivity, specificity, positive predictive value, negative predictive value and accuracy of 96.2%, 100%, 100%, 66.7 and 96.5%, respectively. No immediate complications or delayed life-threatening events were observed.

Conclusion Percutaneous biopsy of metabolically active abdominal and pelvic lesions with ARA assistance is a technically feasible, safe and accurate method for pathological diagnosis with high diagnostic performance. PET-guided biopsy is highly practical and useful in patients, especially in those with a previous inconclusive biopsy.

Keywords Automated robotic arm (ARA) assistance · ^{18}F-FDG PET/CT-guided biopsy · Diagnostic performance · Abdominal and pelvic lesions

✉ Bhagwant Rai Mittal
brmittal@yahoo.com

[1] Department of Nuclear Medicine and PET/CT, Post Graduate Institute of Medical Education and Research, Chandigarh 160012, India

[2] Department of Pathology, Post Graduate Institute of Medical Education and Research, Chandigarh, India

[3] Department of Hemato-Oncology, Post Graduate Institute of Medical Education and Research, Chandigarh, India

[4] Department of Surgery, Post Graduate Institute of Medical Education and Research, Chandigarh, India

[5] Department of Rheumatology, Post Graduate Institute of Medical Education and Research, Chandigarh, India

Introduction

Histopathological evaluation of abdominal and pelvic lesions is essential in deciding on the proper management. Open surgical biopsy used to be a standard procedure for obtaining the tissue sample for histopathology, but it is invasive and is associated with more complications and morbidity [1]. Image-guided percutaneous biopsy is currently more widely accepted as it is minimally invasive and is associated with fewer complications. CT-guided biopsy is versatile and can be used for sampling of superficial as well as deep abdominal lesions with varying diagnostic performance depending upon the target organ and type of needle used [2–4]. ^{18}F-FDG PET/CT provides both metabolic and anatomical details and its use has

therefore been suggested to improve the diagnostic yield of image-guided biopsy [5].

FDG uptake in tumour cells is dependent on enhanced glycolysis and tumour hypoxia which activates the anaerobic glycolytic pathways. FDG PET/CT helps in the early detection of mitotic disease before anatomical changes are evident; it also helps differentiate viable tumour from posttreatment changes within the tumour [6]. However, FDG is relatively nonspecific for malignancy and many nonmalignant conditions (i.e. inflammatory and infective processes) also show FDG avidity, and this adversely affects overall specificity [7]. Therefore, to determine the exact nature of an FDG-avid lesion, percutaneous biopsy may be required before treatment planning.

Recently PET/CT-guided biopsy has gained importance in clinical oncology practice and patient evaluation at various stages of the disease. Some studies have used previously acquired PET images for coregistration with intraprocedural CT images with the help of software fusion or by visual interpretation [8–11]. However, discrepancies in time and space between previously acquired PET images and intraprocedural CT images may lead to placement of the needle tip in a nonviable portion of the tumour and false-negative results. A few recent studies have explored the feasibility of real-time PET-guided biopsy with a fluoroscopic imaging system and have shown high accuracy [9, 12].

The use of robot-assisted image-guided needle placement, tissue sampling, and therapy planning in the field of interventional radiology is evolving rapidly [13]. The role of real-time intraprocedural robotic arm-navigated PET/CT-guided sampling of abdominal or pelvic lesions has not yet been explored. The aim of the present study was to evaluate the feasibility, safety and diagnostic performance of PET/CT-guided sampling of FDG avid abdominal and pelvic lesions with automated robotic arm (ARA) probe assistance.

Materials and methods

Patient population

A total of 114 patients (75 men, 39 women; median age 53 years, mean ± SD 51.3 ± 14.7 years, range 18–90 years) were included prospectively for the sampling of FDG-avid abdominal and pelvic lesions from October 2014 to December 2017. The participating patients provided written informed consent for PET-guided biopsy. The procedure details, associated potential risks and benefits, and other available alternatives were explained to all the participants. Pertinent ethical guidelines were followed for the present study with approval from the ethics review board. All the patients had clinical indications for percutaneous sampling and showed FDG-avid lesions in the abdomen or pelvis on ^{18}F-FDG PET/CT imaging. Coagulation profiles were in accordance with Society of Interventional Radiology guidelines and were obtained 24 h before the procedure [14].

FDG PET/CT imaging

Whole-body images were acquired using a dedicated PET/CT scanner (Discovery STE16 or 710; GE Medical Systems, Milwaukee, WI, USA) after intravenous administration of 300–370 MBq of ^{18}F-FDG. After reviewing the whole-body images, the course of the needle was planned based on the FDG avidity and anatomical location of the lesion, and its proximity to vital organs. The biopsy procedures were performed 3 to 4 h after the diagnostic scan on the same day and using same scanner.

CT and PET parameters for PET/CT-guided intervention

CT imaging parameters during the intervention were 120 kVp, 40 mA, 0.8 s rotation time, and 27.50 mm^2 per rotation with a display field of view of 70 mm. Images were reconstructed at a slice thickness of 1.25 mm using a 512 × 512 matrix. PET images were reconstructed using a 128 × 128 matrix and an iterative ordered subsets expectation maximization (OSEM) algorithm.

Automated robotic arm (ARA) system and work-flow

The ARA workstation (ROBIO-EX; Perfint Healthcare Pvt. Ltd., Chennai, India) is a robotic positioning device (Fig. 1) for fast and accurate targeting of a lesion in PET/CT-guided biopsy. It can be used to target deep lesions requiring orbital, craniocaudal or both angulations. After defining the needle path, patients were positioned and immobilized on a vendor-provided vacuum-assisted immobilizer bed on the PET/CT table. The device was docked on the floor panels installed to the sides of the PET/CT gantry bed on the basis of the planned trajectory. The PET/CT scan of the region of interest was acquired, and DICOM images transferred to the ARA workstation. The desired image slice was chosen on the ARA console and the angle and needle path were determined by defining the target point on the lesion surface and entry point (point of insertion) on the skin considering its relationship with nearby vital organs. The execution command was given to the ARA device to automatically position the robotic arm in a specific orientation corresponding to the planned access path following the procedure previously described in detail by Radhakrishnan et al. [15].

The biopsy procedures were performed under local anaesthesia (1% lidocaine) using strict surgical asepsis. The needle adaptor was placed in the guide probe of the robotic arm positioned in its specific orientation. A suitable

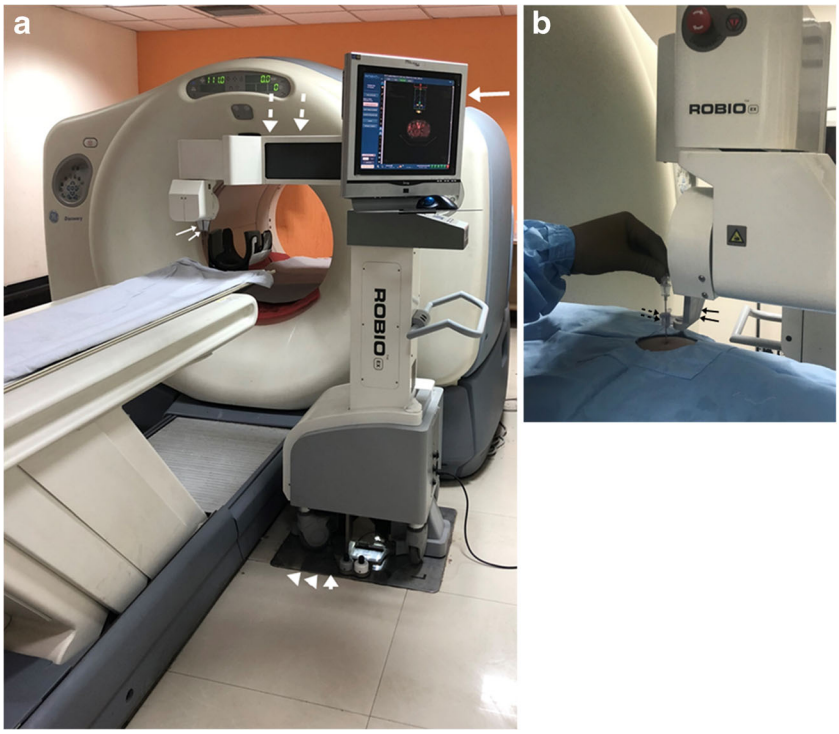

Fig. 1 Photographs of the automated robotic arm system. **a** The system docked on the floor panel (*white arrowheads*) to the side of the PET/CT bed, the console for biopsy planning (*white arrows*), the movable arm of the system (*dashed white arrows*) and the guide probe for placing the needle adaptor. **b** Close-up of the needle adaptor (*dashed black arrows*) placed in the guide probe (*black arrows*) for biopsy needle placement in the target lesion

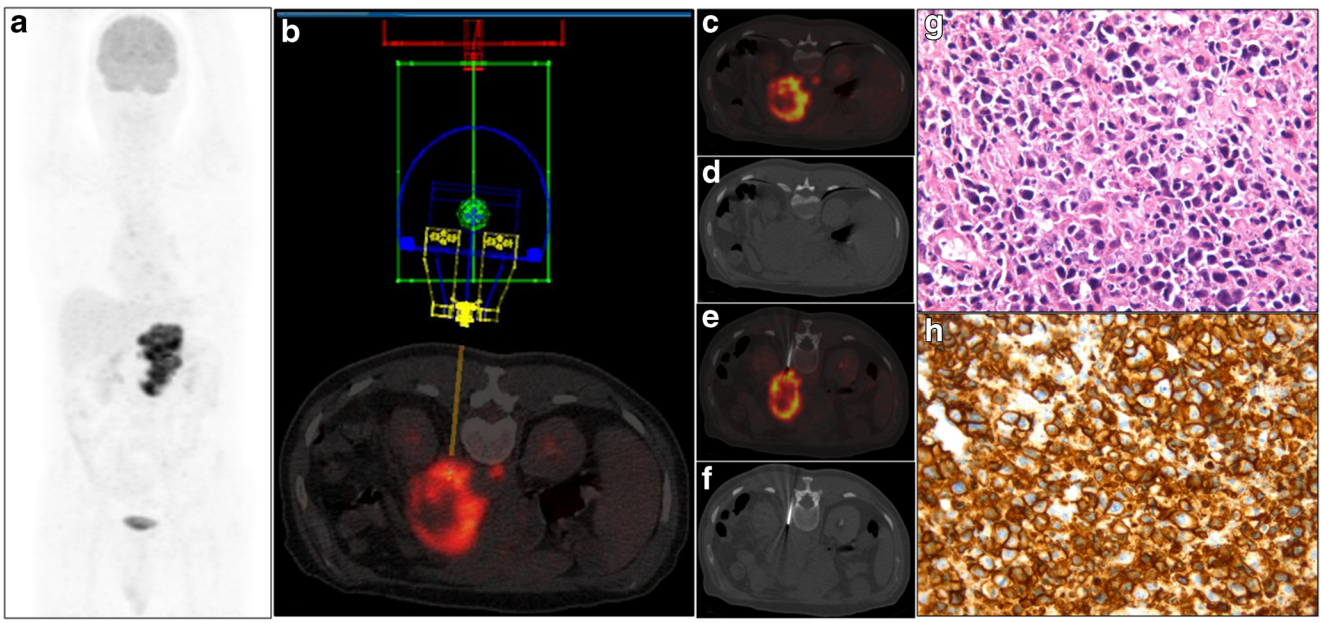

Fig. 2 A 72-year-old man with a treated splenic marginal zone lymphoma presented with retroperitoneal lymphadenopathy and an inconclusive CT-guided biopsy. **a**, **c**, **d** FDG PET/CT imaging shows an FDG-avid abdominal lesion on the maximum intensity projection image (**a**), and an FDG-avid lesion (SUVmax 23.6) in the retroperitoneum with central necrosis on the fused axial PET/CT image (**c**) and the corresponding axial CT image (**d**). **b**, **e**, **f** The fused PET/CT image (**b**) shows the planned trajectory on the ARA console (**b**) and the biopsy needle positioned within the FDG-avid part of the lesion (**e**, **f**). **g–j** Histopathological photomicrographs show large atypical lymphoid cells with background nuclear debris (**g** H&E, ×400) and CD20 positivity (**h** CD20 immunostain, ×400) suggestive of non-Hodgkin's lymphoma

coaxial biopsy system (18G co-axial; Bard Mission; Bard Biopsy, Tempe, AZ, USA) was manually advanced to the target lesion by the interventionist through the guide probe of the robotic arm. After positioning the coaxial needle at the planned depth (as determined by the ARA console) the real-time position of the coaxial needle was confirmed by acquiring a low-dose check CT scan (40 mA) that was fused with the PET images obtained before the procedure. Three-dimensional position-sensitive position coupling of the ARA system with the immobilizer bed and PET/CT scanner ensured effective image fusion. If there was any patient movement during the procedure, a single-bed PET/CT scan was acquired to reconfirm the position of the needle.

After confirming the position of the coaxial needle (Figs. 2, 3 and 4), the stylet was pulled out, and a semiautomated spring-loaded biopsy gun inserted through the coaxial needle. An adequate number of tissue cores (two to eight) were obtained at a 1 cm or 2 cm stall of the biopsy gun during each procedure depending on the size of the lesion and relationship with vital organs. After completion of the procedure, the biopsy site was compressed manually for at least 5 min to achieve haemostasis.

A low-dose check CT scan was acquired after completion of the procedure to look for any immediate complications, and patients were kept under observation for at least 2 to 4 h, and vital signs were measured. The core biopsy/tissue was fixed in 10% formalin and sent for pathological examination. Biopsies were considered technically successful if sufficient tissue was obtained to make a definitive pathological diagnosis. They were considered inconclusive if insufficient tissue was obtained to make a diagnosis, and nonrepresentative if the tissue was not from the target lesion.

The results of the guided biopsies were compared with the composite diagnosis based on pathology, and clinical and/or radiological follow-up. The results were considered true-positive (TP) if histopathology confirmed malignancy or benign pathology. true-negative (TN) if there was no evidence of disease on pathology and even on follow-up, false-positive (FP) if histopathology falsely revealed another pathology,

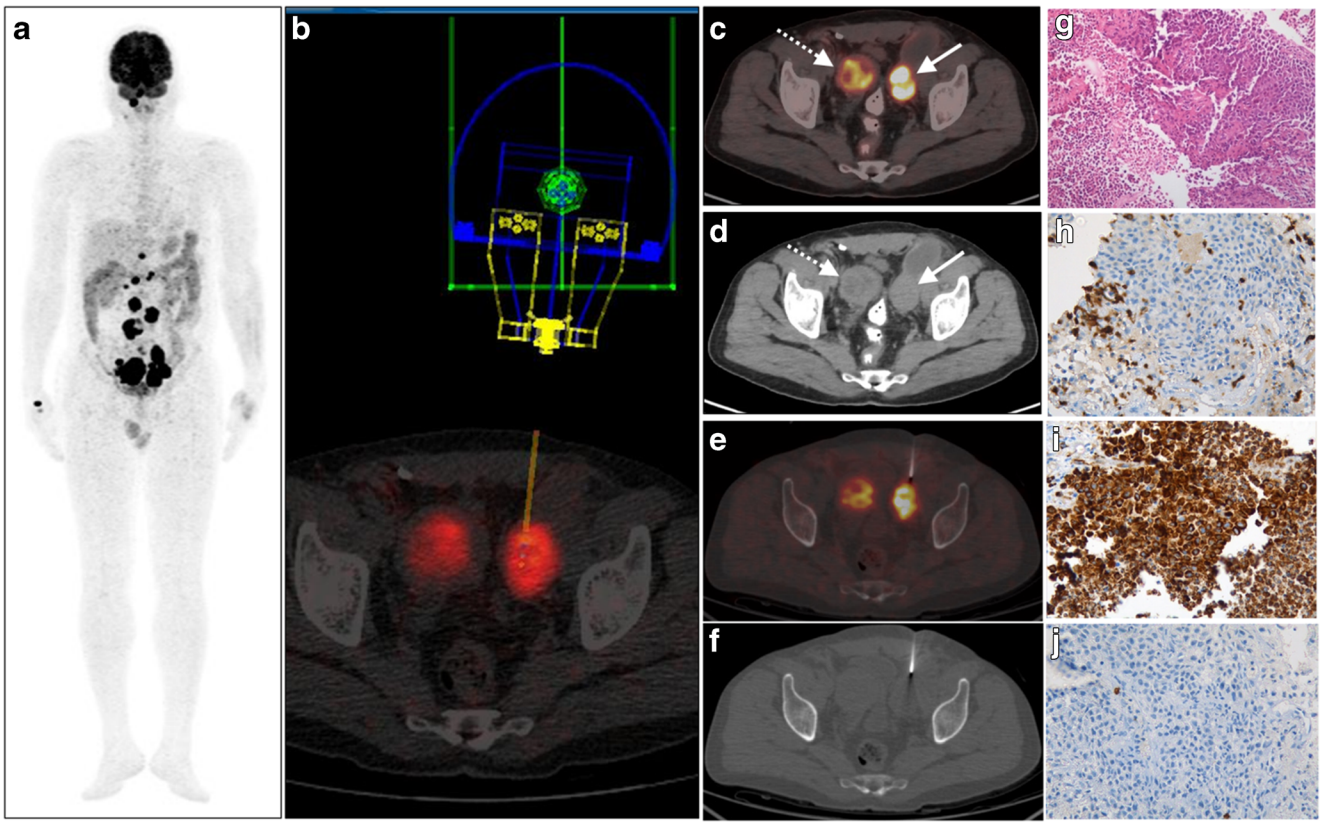

Fig. 3 A 58-year-old man presented with progressive inguinal swelling. **a**, **c**, **d** PET/CT imaging shows FDG-avid lesions in the retroperitoneum and iliac regions on the maximum intensity projection PET image (**a**), and enlarged lymph nodes with necrosis and heterogeneous FDG uptake (*dotted arrows*) on the axial fused PET/CT image (**c**) and the corresponding axial contrast-enhanced CT image (**d**). **b**, **e**, **f** The fused PET/CT image shows the planned trajectory on the ARA console(**b**), and the biopsy needle positioned within the FDG-avid lesion (**e**, **f**). **g**–**j** Histopathology photomicrographs show sheets of mature and immature plasma cells (**g**) with necrosis in the background (H&E, ×400), positive for CD38 (**h** CD38 immunostain, ×400), but negative for CD20 (**I** CD20 immunostain, ×400) and CD3 (**j** CD3 immunostain, ×400), thus allowing a definitive diagnosis of plasmacytoma

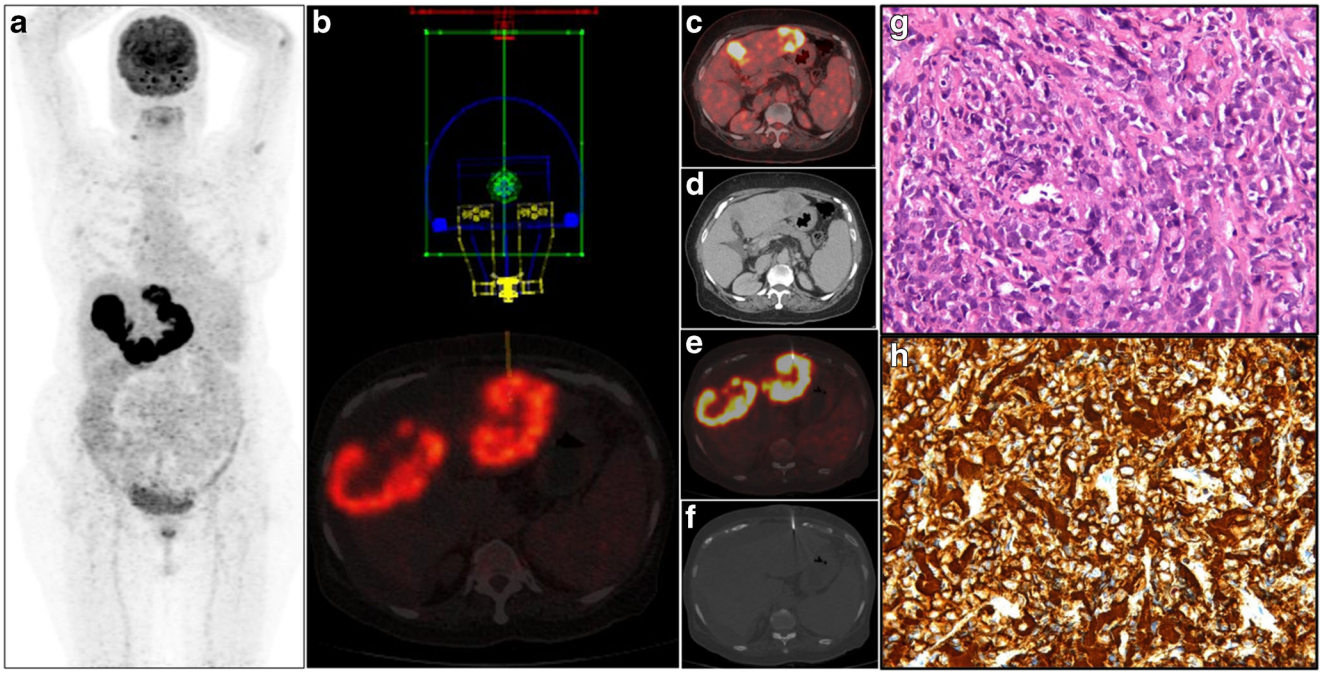

Fig. 4 A 62-year-old woman presented with abdominal pain that had persisted for 1 month. Ultrasonography was suggestive of multiple liver lesions suspicious for hepatocellular carcinoma. **a**, **c**, **d** FDG PET/CT imaging shows an FDG-avid lesion in the right hypochondrium on the maximum intensity projection image(**a**), and FDG-avid hypodense lesions with central necrosis on the axial fused PET/CT image (**c**) and the corresponding contrast-enhanced CT image (**d**). **b**, **e**, **f** The left lobe lesion was targeted for biopsy with the planned trajectory on the ARA console (**b**), and the biopsy needle was positioned within the FDG-avid part of the lesion (**e**, **f**). **g**, **h** Histopathology photomicrographs show large atypical lymphoid cells with sclerosis in the background (**g** H&E, ×400), positive for CD20 (**h** CD20 immunostain, ×400) suggestive of diffuse large B-cell lymphoma

and false-negative (FN) if histopathology did not reveal any diagnosis (malignancy or benign disease). Nonrepresentative and inconclusive results were considered FN. The diagnostic performance of the procedure was calculated on the basis of these criteria.

Table 1 Distribution of biopsy sites in 114 patients

Target site	No. of lesions
Abdominal and retroperitoneal lesions	
Liver	15
Spleen	1
Stomach	1
Mesenteric lymph node/mass	16
Gallbladder fossa	2
Omental/peritoneal deposit	6
Kidney	7
Pancreas	9
Psoas	3
Adrenal	3
Paraaortic/retroperitoneal lymph node	34
Total	97 (85.1%)
Pelvic lesions	
External iliac/internal iliac lymph nodes	14
Common iliac lymph nodes	1
Pararectal deposit	2
Total	17 (14.9%)

Results

The posterior approach (Fig. 1) was used in 56 patients (retroperitoneal lymph nodes in 34, renal lesions in 7, perinephric deposit in 1, adrenal lesions in 3, liver lesions in 10, and spleen lesions in 1) with the patient lying in the prone position. The anterior approach (Figs. 2 and 3) was used in the remaining 58 patients with the patient lying in the supine position. The mean lesion size was 2.99 ± 0.85 cm (range 1.5–6.2 cm), and the mean access path length was 6.02 ± 2.3 cm (range 2.0–12.5 cm). Of the 114 patients, 71 (62.3%) had a previous image-guided tissue biopsy. The biopsy sites are listed in Table 1.

Histopathological findings

FDG PET/CT-guided biopsy of the abdominal and pelvic lesions was technically successful in 110 of the 114 patients (96.5%) and confirmed the pathological diagnosis. In the remaining four patients the pathology results were either inconclusive (one patient), or the sample was nonrepresentative (three patients). Of the 110 lesions, 82 were malignant, 20 were benign, and 8 showed no residual disease and minimal residual FDG uptake on the end-of-treatment PET/CT scan.

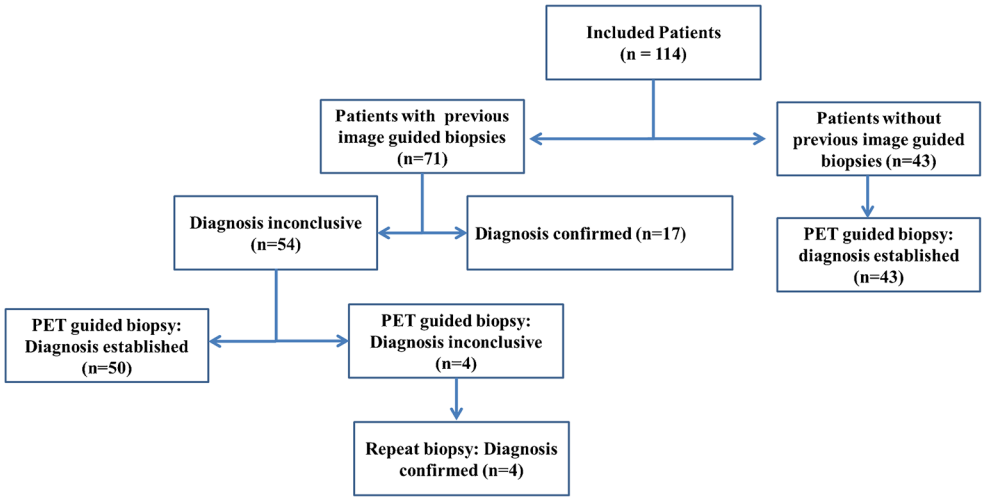

Fig. 5 Structured flow diagram showing the pathological findings in patients who underwent PET/CT-guided biopsy of FDG-avid abdominal and pelvic lesions

In 54 of 71 patients (76.1%) with a previous inconclusive image-guided biopsy, PET-guided biopsy established the pathological diagnosis in 50 of these 54 patients, and four patients underwent repeat biopsy because of a nonrepresentative sample or inconclusive biopsy (two with lymphoma, one with metastatic adenocarcinoma, and one with pancreatic carcinoma). These results are summarized as a flow diagram in Fig. 5. The pathology results are summarized in Table 2. Of the 71 patients with proven pathology, 17 (23.9%) underwent PET-guided biopsy to rule out Richter's transformation in chronic lymphocytic leukaemia (three patients), to determine the metastatic status of proven adenocarcinoma (eight patients), for immunohistochemistry of round cell tumour (four patients), to determine the perinephric deposit status in multiple myeloma (one patient), and to determine the level of mitotic activity in germ cell tumour (one patient; mitotic disease was revealed on histopathology; Table 3).

The remaining 43 patients with no previous biopsy underwent PET-guided biopsy, 20 with clinical suspicion of

Table 2 The clinical and histopathological diagnoses in 54 patients with inconclusive conventional image-guided biopsy

Clinical suspicion or diagnosis	PET-guided biopsy results	Number	Comments
Lymphoma ($n = 26$)	Lymphoma	23	
	Plasmacytoma	1	
	Tuberculosis	1	
	Nonrepresentative sample	1	Re-biopsy: lymphoma
Primary pancreatic cancer ($n = 5$)	Adenocarcinoma	2	
	High-grade neuroendocrine tumour	1	
	Lymphoma	1	Re-biopsy: pancreatic cancer
	Inconclusive pathology	1	
Pyrexia of unknown origin ($n = 6$)	Lymphoma	2	
	Sarcoidosis	1	
	Histoplasmosis	1	
	Tuberculosis	1	
	Nonrepresentative sample	1	Re-biopsy: lymphoma
Suspected distant metastases ($n = 11$)	Metastatic carcinoma	6	Primary in gallbladder ($n = 3$), lung ($n = 1$), stomach ($n = 1$), thyroid ($n = 1$)
	Lymphoma	1	
	Tuberculosis	2	
	Reactive nodal hyperplasia	1	Benign disease on follow-up
	Nonrepresentative sample	1	Re-biopsy: metastatic endometrial cancer
Neuroendocrine tumour ($n = 3$)	Metastatic adenocarcinoma	1	
	Lymphoma	1	
	Neuroendocrine tumour	1	
Plasmacytoma ($n = 1$)	Plasmacytoma	1	
Hepatocellular cancer ($n = 2$)	Lymphoma	1	
	Cholangiocarcinoma	1	
Total		54	

Table 3 Clinical and histological diagnoses in 17 patients with positive conventional image-guided biopsy, and PET-guided biopsy done to confirm the diagnosis

Clinical diagnosis	PET-guided biopsy results	Number	Comments
Chronic lymphocytic leukaemia ($n = 3$)	Richter's transformation	3	
Multiple myeloma ($n = 1$)	Plasmacytoma	1	Perinephric deposit
Metastases/deposit ($n = 8$)	Metastatic adenocarcinoma: pancreas ($n = 1$), gallbladder ($n = 3$), lung ($n = 2$), endometrium ($n = 1$), breast ($n = 1$)	8	
Round cell tumour ($n = 4$)	Neuroendocrine tumour	2	
	Lymphoma	2	
Germ cell tumour ($n = 1$)	Germ cell tumour	1	
Total		17	

lymphoma, 13 with metastatic disease, 7 with pyrexia of unknown origin, 2 with retroperitoneal sarcoma, and 1 with a paraneoplastic aetiology. The pathology results are summarized in Table 4.

Complications and side effects

All the patients tolerated the biopsy procedure under local anaesthesia. A few patients reported transient pain or showed a minor bleed, but no major life-threatening complications were observed in any of the patients either during or after the procedure. The physician was exposed to an average radiation dose of 0.85 μSv per procedure with a calculated absorbed dose of 425 μSv per year (0.85 μSv per procedure × about ten procedures per week × about 50 working weeks in a year).

Follow-up and the diagnostic performance of PET-guided biopsy

An adequate amount of representative tissue for histopathology was obtained in all but four patients. On clinical or imaging follow-up, none of the patients with a pathological malignant diagnosis or benign disease had an alternative diagnosis. The patients with no pathological evidence of malignancy on follow–up for at least 3 months revealed no active disease. Four patients who had inconclusive or nonrepresentative samples and a strong clinical suspicion of malignancy underwent

Table 4 Clinical and histopathological diagnoses in 43 patients who underwent PET-guided biopsy with no prior CT-guided biopsy

Clinical diagnosis	PET-guided biopsy results	Number	Comments
Lymphoma ($n = 20$)	Lymphoma	7	
	No evidence of disease[a]	8	No disease on follow-up
	Tuberculosis	1	Treated with antitubercular therapy
	Cysticercosis	1	Responded to albendazole therapy
	Reactive hyperplasia	1	Diagnosis confirmed on follow-up
	Diabetic nephropathy	1	Diagnosis confirmed on follow-up
	Chronic pancreatitis	1	Benign confirmed disease on follow-up
Metastatic disease ($n = 13$)	From gallbladder cancer	5	
	From neuroendocrine tumour	2	
	From kidney, rectum, pancreas, lung, prostate and unknown primary (one each)	6	
Pyrexia of unknown origin ($n = 7$)	Tuberculosis	5	Treated with antitubercular therapy
	Hepatitis	1	Benign confirmed disease on follow-up
	Reactive hyperplasia	1	Benign confirmed disease on follow-up
Retroperitoneal sarcoma ($n = 2$)	Malignant fibrometosis	1	
	Lymphoma	1	
Paraneoplastic syndrome ($n = 1$)	Vasculitis	1	Benign confirmed disease on follow-up
Total		43	

[a] End-of-treatment PET/CT revealed minimal residual FDG uptake in the lesions

repeat biopsy for confirmation of diagnostic suspicion (lymphoma in two, pancreatic carcinoma in one, metastatic adenocarcinoma in one).

The diagnostic yield of the procedure was 96.5%. The histopathological results revealed 102 TP findings, no FP findings, 8 TN findings and 4 FN findings. The sensitivity, specificity, positive predictive value, negative predictive value and accuracy of PET/CT-guided biopsy for diagnosing abdominopelvic lesions were 96.2%, 100%, 100%, 66.7 and 96.5%, respectively.

Discussion

The initial imaging modalities for diagnosing a lesion are ultrasonography, CT and MRI. These techniques provide images with specific features that enable characterization of the type of lesion (malignant vs. benign), but small lesions without specific imaging features are difficult to characterize. Similarly, in a heterogeneous lesion, it is difficult to distinguish the malignant from the necrotic areas [16]. In current oncology practice, the management of malignant lesions not only depends on the pathological diagnosis but also requires immunohistochemistry, accurate tumour staging and genetic information which further determine the treatment strategy and risk-adapted individualized therapy [17]. Therefore, a carefully performed biopsy along with immunohistochemistry and genetic analysis is the gold standard to identify the exact nature of lesions. Deep or small lesions in the retroperitoneum and pelvis are not readily accessible for ultrasound-guided sampling. Percutaneous CT-guided needle biopsy is a minimally invasive procedure, provides excellent visualization of the anatomical details and provides safe and accurate access to deep lesions with fewer complications [18, 19]. ^{18}F-FDG PET/CT has shown excellent accuracy in the staging of most cancers and helps avoid inappropriate treatment [20].

Frequently, most of the area of a large tumour mass is necrotic with only a small area being metabolically active. Apart from diagnosis, FDG PET/CT can also help in the detection of the most hypermetabolic region within a lesion, thereby guiding the biopsy to the optimal region of the lesion [16]. Visual or computer-based software fusion of previously acquired PET images with intraprocedural CT images for PET/CT-guided biopsy is time consuming, requires additional computer-based software and lacks temporal resolution [21]. The accurate spatial registration of intraprocedural CT images with previously acquired PET/CT images is not always possible because of differences in patient positioning during PET and CT-guided intervention, and respiratory, cardiac and body part movements which lead to inaccurate tissue retrieval [22]. A few recent studies have investigated the value of intraprocedural PET/CT-guided biopsy using the same scanner and have shown that this technique is feasible with a high diagnostic success rate. The FDG PET/CT acquisitions were done just before the interventional procedure from the hypermetabolic site [12, 23].

The C-arm-assisted or robotic arm-assisted needle placement within a lesion for sampling and treatment planning have shown high accuracy and the procedure is rapidly evolving. Apart from these applications, the procedure may be helpful in targeting lesions that are difficult to approach and may allow reductions in radiation exposure and procedure time [13, 24]. A few recent studies have investigated the value of robotic arm-assisted intraprocedural PET/CT-guided biopsy of thoracic and posttreatment lesions in non-Hodgkin's lymphoma and have shown that the technique is feasible and may help in the accurate targeting of the hypermetabolic portion of the lesions [15, 25]. However, robotic arm-assisted real-time PET/CT-guided biopsy of abdominal and pelvic lesions, and the diagnostic performance of this technique, have not yet been investigated.

In the present study, the entire procedure was performed on the same PET/CT scanner, and the intraprocedural emission and CT images were acquired during the same session. Problems related to spatial registration of previously obtained PET images with intraprocedural CT images, differences in patient positioning and movements of body parts were thus obviated. Additionally, the robotic arm was used for targeting the lesions which again helped in targeting the hypermetabolic part of lesions. The vacuum-assisted patient bed arrester also reduced the movement of body parts during the procedure and enhanced the efficiency of the technique.

In this prospective study, the biopsy needle was placed accurately in the hypermetabolic part of abdominopelvic lesions in all 114 patients, and an accurate diagnostic sample for pathology was obtained in 110 patients. The remaining four patients underwent re-biopsy because of high clinical suspicion, and pathology revealed lymphoma in two, pancreatic cancer in one and metastatic adenocarcinoma in one. In all these four patients the lesions were either very near to a blood vessel or vital organ, or a minimal amount of tissue was obtained to avoid any unnecessary procedure-related complications. In the present study the lesion size (mean ± SD) was 2.99 ± 0.85 cm (range 1.5–6.2 cm). The smallest lesion targeted was an omental nodule measuring 1.5 cm. The ARA helped precisely target small lesions and reduced the procedure time. PET-guided biopsy changed the diagnosis in patients with previous inconclusive image-guided biopsy except in the four patients discussed above. The PET/CT-guided biopsy procedure showed high performance in the pathological diagnosis of abdominal and pelvic lesions. The postintervention inflammatory process may lead to false-positive FDG uptake on PET/CT. PET/CT after a surgical procedure should be delayed by at least 6 weeks to avoid false-positive FDG uptake [26]. Mild FDG uptake may be seen after a previous CT-guided biopsy procedure due to inflammation, and can be

of significance in small lesions. However, in the present study no false-positive pathology was seen on PET/CT-guided biopsy in patients with previous CT-guided intervention.

In this series, despite minimal pain and a small amount of bleeding, most patients tolerated the biopsy procedure very well, confirming that this robotic arm-assisted real-time PET/CT-guided biopsy technique is safe, feasible and practical for abdominal and pelvic lesions, and diagnostic tissue was obtained in most patients (96.5%). No immediate or delayed postprocedural life-threatening complications were seen in any of the patients. The physician was exposed to an average radiation dose of 0.85 μSv with a calculated absorbed dose of 425 μSv per year, which is significantly less than the limit prescribed by IRCP 103 [27]. The radiation exposure limits were similar to the exposure doses measured by Lakhanpal et al. [28].

Although PET/CT-guided biopsy of abdominal and pelvic lesions demonstrated high diagnostic performance, it also had some limitations. The procedure is time consuming leading to high occupancy of the PET/CT system. Secondly, small lesions and those in proximity to vital organs or blood vessels are not easy to target and this may lead to inappropriate sampling or procedure-related complications. Additionally, the lesions sampled were not checked ex vivo for radioactivity. Checking radioactivity in biopsy samples may be a novel approach to control sampling effectiveness to discriminate between viable and necrotic tissue.

The diagnostic yield in the present study is comparable to the 100% diagnostic yield of ARA-assisted PET/CT-guided biopsy found by Radhakrishnan et al. in 25 patients with thoracic and mediastinal lesions and previous nondiagnostic conventional biopsy [15]. Respiratory movement, a deep location and proximity to large vessels may cause difficulty in sampling of smaller lesions in the mediastinum and abdomen. Despite these difficulties, robotic arm-assisted PET-guided intervention leads to appropriate placement of the needle within the target lesion. We consider that PET/CT-guided interventions are of great help in the management of oncological patients and that a dedicated PET/CT scanner with an interventional suite is a necessary resource for patient management.

Conclusion

ARA-assisted ^{18}F-FDG PET/CT-guided percutaneous real-time biopsy of metabolically active abdominal and pelvic lesions is a technically feasible, safe and accurate method for pathological diagnosis. PET-guided biopsies were highly practical and useful in patients, especially in those with a previous inconclusive biopsy. The technique also helps in the accurate staging of lesions with minimal residual FDG uptake on posttreatment PET/CT.

Funding The present study did not receive any funding.

Compliance with ethical standards

Conflicts of interest None.

Ethical approval All procedures performed in studies involving human participants were in accordance with the ethical standards of the institutional and/or national research committee and with the principles of the 1964 Declaration of Helsinki and its later amendments or comparable ethical standards.

Informed consent Informed consent was obtained from all individual participants included in the study.

References

1. Hopper KD. Percutaneous, radiographically guided biopsy: a history. Radiology. 1995;196:329–33.
2. Guimarães AC, Chapchap P, de Camargo B, Chojniak R. Computed tomography-guided needle biopsies in pediatric oncology. J Pediatr Surg. 2003;38(7):1066–8.
3. Chojniak R, Isberner RK, Viana LM, Yu LS, Aita AA, Soares FA. Computed-tomography guided needle biopsy: experience from 1, 300 procedures. Sao Paulo Med J. 2006;124(1):10–4.
4. Arnolli MM, Hanumara NC, Franken M, Brouwer DM, Broeders IA. An overview of systems for CT- and MRI-guided percutaneous needle placement in the thorax and abdomen. Int J Med Robot. 2015;11(4):458–75.
5. Kumar R, Halanaik D, Malhotra A. Clinical applications of positron emission tomography-computed tomography in oncology. Indian J Cancer. 2010;47(2):100–19.
6. Khan N, Islam MM, Mahmood S, Hossain GA, Chakraborty RK. 18F-fluorodeoxyglucose uptake in tumor. Mymensingh Med J. 2011;20(2):332–42.
7. El-Haddad G, Alavi A, Mavi A, Bural G, Zhuang H. Normal variants in [18F]-fluorodeoxyglucose PET imaging. Radiol Clin North Am. 2004;42(6):1063–81, viii. https://doi.org/10.1016/j.rcl.2004.07.003.
8. Paparo F, Piccazzo R, Cevasco L, Piccardo A, Pinna F, Belli F, et al. Advantages of percutaneous abdominal biopsy under PET-CT/ultrasound fusion imaging guidance: a pictorial essay. Abdom Imaging. 2014;39(5):1102–13.
9. Cerci JJ, Tabacchi E, Bogoni M, Delbeke D, Pereira CC, Cerci RJ, et al. Comparison of CT and PET/CT for biopsy guidance in oncological patients. Eur J Nucl Med Mol Imaging. 2017;44(8):1269–74.
10. Tatli S, Gerbaudo VH, Mamede M, Tuncali K, Shyn PB, Silverman SG. Abdominal masses sampled at PET/CT-guided percutaneous biopsy: initial experience with registration of prior PET/CT images. Radiology. 2010;256(1):305–11.
11. Cerci JJ, Tabacchi E, Bogoni M. Fluorodeoxyglucose-PET/computed tomography-guided biopsy. PET Clin. 2016;11(1):57–64.
12. Guo W, Hao B, Chen HJ, Zhao L, Luo ZM, Wu H, et al. PET/CT-guided percutaneous biopsy of FDG-avid metastatic bone lesions in patients with advanced lung cancer: a safe and effective technique. Eur J Nucl Med Mol Imaging. 2017;44(1):25–32.
13. Tam AL, Lim HJ, Wistuba II, Tamrazi A, Kuo MD, Ziv E, et al. Image-guided biopsy in the era of personalized cancer care: proceedings from the Society of Interventional Radiology Research consensus panel. J Vasc Interv Radiol. 2016;27(1):8–19.
14. Patel IJ, Davidson JC, Nikolic B, Salazar GM, Schwartzberg MS, Walker TG, et al. Consensus guidelines for periprocedural management of coagulation status and hemostasis risk in percutaneous image-guided interventions. J Vasc Interv Radiol. 2012;23(6):727–36.

15. Radhakrishnan RK, Mittal BR, Gorla AKR, Basher RK, Sood A, Bal A, et al. Real-time intraprocedural (18)F-FDG PET/CT-guided biopsy using automated robopsy arm (ARA) in the diagnostic evaluation of thoracic lesions with prior inconclusive biopsy results: initial experience from a tertiary health care centre. Br J Radiol. 2017;90(1080):20170258.
16. Hain SF, O'Doherty MJ, Bingham J, Chinyama C, Smith MA. Can FDG PET be used to successfully direct preoperative biopsy of soft tissue tumours? Nucl Med Commun. 2003;24:1139–43.
17. Patel AS, Soares B, Courtier J, Mackenzie JD. Radiation dose reduction in pediatric CT-guided musculoskeletal procedures. Pediatr Radiol. 2013;43:1303–8.
18. Azrumelashvili T, Mizandari M, Magalashvili D, Dundua T. Imaging guided percutaneal core biopsy of thoracic bone and soft tissue lesions – technique and complications. Georgian Med News. 2016;250:17–24.
19. Tomozawa Y, Inaba Y, Yamaura H, Sato Y, Kato M, Kanamoto T, et al. Clinical value of CT-guided needle biopsy for retroperitoneal lesions. Korean J Radiol. 2011;12(3):351–7.
20. Gallamini A, Zwarthoed C, Borra A. Positron emission tomography (PET) in oncology. Cancer (Basel). 2014;6(4):1821–89.
21. Abi-Jaoudeh N, Kruecker J, Kadoury S, Kobeiter H, Venkatesan AM, Levy E, et al. Multimodality image fusion-guided procedures: technique, accuracy, and applications. Cardiovasc Intervent Radiol. 2012;35:986–98.
22. Rajagopal M, Venkatesan AM. Image fusion and navigation platforms for percutaneous image-guided interventions. Abdom Radiol (NY). 2016;41(4):620–8.
23. Aparici CM, Aslam R, Win AZ. Initial experience of utilizing real-time intra-procedural PET/CT biopsy. J Clin Imaging Sci. 2014;4:54.
24. Jiao D, Xie N, Wu G, Ren J, Han X. C-arm cone-beam computed tomography with stereotactic needle guidance for percutaneous adrenal biopsy: initial experience. Acta Radiol. 2017;58(5):617–24.
25. Radhakrishnan RK, Mittal BR, Basher RK, Prakash G, Malhotra P, Kalra N, et al. Post-therapy lesions in patients with non-Hodgkin's lymphoma characterized by 18F-FDG PET/CT-guided biopsy using automated robotic biopsy arm. Nucl Med Commun. 2018;39:74–82.
26. Boellaard R, Delgado-Bolton R, Oyen WJ, Giammarile F, Tatsch K, Eschner W, et al. European Association of Nuclear Medicine (EANM). FDG PET/CT: EANM procedure guidelines for tumour imaging: version 2.0. Eur J Nucl Med Mol Imaging. 2015;42(2):328–54.
27. International Commission on Radiological Protection. The 2007 recommendations of the International Commission on Radiological Protection. ICRP publication 103. Ann ICRP. 2007;37:1-332. https://doi.org/10.1016/j.icrp.2007.10.003.
28. Lakhanpal T, Mittal BR, Kumar R, Watts A, Rana N, Singh H. Radiation exposure to the personnel performing robotic arm-assisted positron emission tomography/computed tomography-guided biopsies. Indian J Nucl Med. 2018;33:209–13.